Title: *Fuel constraints not fire weather conditions limit fire behavior in reburned boreal forests*

Authors: Katherine Hayes[1,2], Chad Hoffman[3], Rod Zin[4], Justin Ziegler[3,5], Brian Buma[1,6]

Corresponding author: hayesk@caryinstitute.org

Abstract

Fire frequency in boreal forests has increased via longer burning seasons, dryer conditions, and higher temperatures. However, fires have historically self-regulated via fuel limitations, mediating the effects of changes in climate and fire weather. Early post-fire boreal forests (stands 10-15 years postfire) are often dominated by mixed conifer-broadleaf or broadleaf regeneration, which are considered less flammable due to the higher foliar moisture of deciduous trees and shrubs compared to their more intact conifer counterparts. However, the strength of self-regulation in the context of changing fire weather and the emergence of novel forest communities and structures remains unclear. We quantified fuel composition, abundance, and structure in burned and reburned forests in Interior Alaska and then created virtual forest landscapes and simulated fire behavior using the Wildland-Urban Interface Fire Dynamics Simulator (WFDS) to understand how these unique patterns of fuel influence the rate and sustainability of fire spread and fuel consumption. We sampled forests that burned once, twice or three times in short intervals of 50 years or less to capture the gradient of forest composition and

[1] Department of Integrative and Systems Biology, University of Colorado Denver, Campus Box 171 P.O. Box 173364 Denver, CO 80217-3364
[2] Present: Cary Institute of Ecosystem Studies, 2801 Sharon Turnpike, Millbrook NY 12545
[3] Department of Forest and Rangeland Stewardship, Colorado State University, 1401 Campus Delivery Fort Collins, CO 80523-1401
[4] Los Alamos National Laboratory, P.O. Box 1663 Los Alamos, NM 87545
[5] Present: Aster Global Environmental Solutions, 3800 Clermont St. NW North Lawrence, OH 44666
[6] Present: Environmental Defense Fund, 2060 Broadway Suite 300 Boulder, CO 80302

structure present in forests regenerating after multiple fire events. In forests that had experienced one fire, extreme fire weather conditions allowed for sustained fire spread, suggesting that intense fire conditions can enable short-interval events. However, fire spread was not sustained in thrice-burned regenerating forests, where regeneration was often dense but more clumped, and thus less connected, separated by patches of bare soil. Fire traveled an average of 50 m into thrice-burned forests before dying out, even under extreme fire weather conditions. This work suggests that fire spread may be possible in once-burned forests under extreme fire weather conditions but may be more limited in less connected and less fuel abundant thrice-burned regenerating forests, at least within the 10-15 year window post-fire.

Keywords: Fire, Boreal Forests, Fire Behavior, Self-Regulation, Fuel

1. Introduction

Reburning is increasing in Interior Alaska due to warming temperatures, longer fire seasons (Lund et al., 2023), increased lightning (Veraverbeke et al., 2017) and drier conditions (Buma et al., 2022). Historically, fires were infrequent (Hoecker and Higuera, 2019) and high-severity (complete canopy mortality), enforcing a ‘legacy lock’ on forest composition that allowed conifers, such as black spruce (*Picea mariana*), to dominate (Johnstone et al., 2010). Reburns (two fires in an interval of 50 years or less in the boreal) and continued reburning (three or more fires in an interval of 150 years or less) drive stand-level transitions from conifer-dominated forests to deciduous shrublands and grasslands (Hayes and Buma, 2021; Johnstone and Chapin, 2006). Boreal deciduous communities have historically been less capable of igniting and carrying fire spread (Barrett et al., 2016) due to higher foliage moisture (Kelly et al., 2013) of species like birch and aspen. Following that logic, an increased presence of deciduous species across boreal forests could enable negative feedbacks to future fire (Brubaker et al., 2009), also referred to as ‘self-regulation’ (Hart et al., 2019; Parks et al., 2015). However, the strength, reliability, and potential duration of self-regulation remains unclear, given two factors: one, that ongoing reburning is shifting community composition outside historic norms and two, extreme fire weather conditions may overwhelm foliar moisture constraints. To better evaluate the potential strength of deciduous self-regulation in boreal forests under warming conditions, we need a better understanding of fire behavior in emerging deciduous regeneration.

Fire behavior is a product of how a fire responds to the interactions of fuel, weather and topography. While topography plays an important role in fire behavior in forests of Interior Alaska, here we focus on how changing fuel and changing fire weather conditions may alter how deciduous stands burn.

Both fuel abundance and fuel arrangement are important factors for fire behavior and both are controlled by forest structure and composition (Atchley et al., 2021; Parsons et al., 2017). In boreal Interior Alaska, forests have been remarkably stable for thousands of years under an infrequent, high severity fire regime (Kelly et al., 2013), which promoted black spruce dominance across the region. Deciduous communities were present (Higuera et al., 2018) but limited and predominantly dominated by birch (*Betula neoalaskana*). However, paleoecological community types, on which the description of a negative feedback is partly based, are not analogous to modern emerging communities in Alaska: mid-Holocene boreal deciduous environments were dominated by birch (Higuera et al., 2008; Kelly et al., 2013) while recent studies have found alder (*Alnus crispa*), aspen (*Populus tremuloides*), and even willow (*Salix* spp.) in dominant quantities in modern boreal forests after reburning (Hayes and Buma, 2021; Johnstone et al., 2020). Early observations of regenerating deciduous forests in Interior Alaska demonstrate that forest structure changes distinctively across a 1-3 short-interval fire gradient: three burns result in a more open, clumped spatial distribution of trees via increased presence of willow and aspen (Hayes and Buma, 2021). Tree structure plays an important role in shaping fuel distributions (Eckdahl et al., 2022; Hély et al., 2000): changing forest structure and composition alters fire behavior via changes to specific fire behavior variables, such as ignitability, spread intensity, and wind flow. In addition, deciduous species are faster growing, outpacing black spruce regeneration (Mack et al., 2021) which could lead to greater fuel abundance. Currently, we lack modern empirical data on the spatial distribution and abundance of fuels in emerging deciduous stands, limiting our ability to make informed hypotheses about potential fire behavior.

In addition, fire weather conditions are changing in Alaska (Lund et al., 2023) in ways outside the norms displayed in historic or paleoecological analogs. Extreme fire seasons (Turquety et al., 2007) may become the norm via increasingly warm and dry summers (Balshi et al., 2009; Lund et al., 2023). Importantly, in 2004 and 2005 under extreme fire weather conditions, spruce and mature deciduous stands burned at similar frequencies (Kasischke et al., 2010), suggesting foliar moisture constraints could be overridden. In addition, studies of recent reburning in Alaska found the effects of self-regulation are strongest within the first decade after fire but begin to decay within 10 to 20 years (Buma et al., 2022). The combined impact of novel community types, more open stand structures, and extreme climate-driven fire weather may enable fire to overcome previous self-regulation thresholds. Understanding the future characteristics of boreal fire regimes requires evaluating the combined role of shifts in community type, forest structure, and fire weather conditions and their potential cumulative impact on future fire behavior.

One challenge in understanding potential future fire behavior is the intrinsic novelty of emerging forest types: most of our tools for understanding and predicting fire behavior depend on norms and relationships determined by historic observations (i.e., standardized indices of fuel types, Stocks et al., 1989). Emerging forest types with structures and compositions that differ from historic norms require models that can simultaneously test changing fire weather with shifts in fuel characteristics and stand structures.

Physics-based wildland fire behavior modeling can be used to explore potential fire behavior even in systems with novel fuel characteristics (Hoffman et al., 2018). One such model is the Wildland-Urban Interface Fire Dynamics Simulator (WFDS version 9977), a physics-based fire behavior model that represents individual ecosystem components and the interactions of combustion with the atmosphere. WFDS models fuel composition and structure in three dimensions, accounting for bulk density, surface area to volume ratio, heat of combustion, and fuel moisture. WFDS has a wide range of applicability (Mell et al., 2010), including the exploration of novel fire behavior across complex fuel structures such as the Wildland-Urban-Interface (Mell et al., 2011), bark beetle-infested forests (Hoffman et al., 2012, 2013), transitions between homogenous conifer forests and mixed conifer-deciduous forests (Ziegler et al., 2021), and fuel hazard reduction and restoration treatments (Ritter et al., 2022; Ziegler et al., 2020).

The lack of relevant information on emerging deciduous forests and their relationship with fire provides an ideal and timely opportunity to apply a physics-based model to questions related to fire behavior and fire self-regulation, which are topics of considerable importance for future boreal forest stability. Our objective was to evaluate how fuel composition, fuel density, and distribution change with increasing short-interval reburns to explore potential fire behavior across a gradient of fuel and weather conditions. In contrast to previous studies that examined the distribution and abundance of fuel elements after a single fire event, here we assessed fuel characteristics in boreal stands that have experienced one to three short-interval sequential fires. We hypothesize that fuel connectivity and abundance will initially increase with additional fires but decrease after three short-interval fires as reburns continue to consume fuel. In addition, we expect that potential fire behavior may increase as a result of successive reburns and community type changes, given the difference in forest structure created by different dominating vegetation. Finally, we predicted that extreme fire weather conditions (high winds and low fuel moisture) may produce novel potential fire behavior in reburned stands, potentially overwhelming fuel constraints (i.e., connectivity or abundance) to burn stands that would not burn otherwise.

2. Materials and Methods

2.1 Study Area

To investigate how reburns alter the spatial distribution of fuel, we sampled spatial patterns of fuel abundance and distribution at two locations in Interior Alaska. Each site experienced 1-3 fires within >30-year intervals, and between both locations, 42 plots were randomly established within burn perimeters 100m apart and a minimum of 50 m from roads. Eight additional plots were established in the unburned perimeters as references for the assumed prefire conditions.

2.2 Field Sampling

To quantify fuel abundance in reburns, we measured dead down woody debris fuel loads (DWD, dead wood lying or standing below <45-degree angle) using two 28-m transects (Brown, 1974) radiating from the center of each 20m-by-20m plot. We recorded the diameter, species, presence of charred material, and decay class of 1000-hour fuels across the full transect and counted <3 cm fine debris across subsets (1-hr = 2m, 10-hr = 5 m, 100-hr = 15m). Total fuel loading (tons/ha) was calculated by converting DWD field data into estimates of mass per area (grams per meter) following Brown (1974). We measured mass of understory fuels (grass, litter, and shrubs) by harvesting randomly located 1 x 1 m subplots, drying vegetation for 48 hours at 50° C and then weighing. We measured surface fuel depth by recording height of the tallest vegetation (live and dead) connected continuously to the forest floor across 2-meter increments of the transect. To capture standing live and dead fuel abundance, we measured height and diameter at breast height (DBH 1.37 m) of standing live and dead trees in each plot in 200 m^2 randomly selected subsections and scaled to produce estimates of tree density. We estimated total biomass of each species using a suite of local species-specific allometric equations (see

Appendix: Table S1 for specifics; Binkley, Lousier, Cromack, 1984; Bond-Lamberty et al., 2002).

To calculate the spatial dispersion of standing fuel elements, we measured the distance to the nearest tree of each species present in the plot from each of the 10 sampling cubes. We used the resulting measurements of a random point for each tree species to calculate Eberhardt's index, a metric of dispersion based on random point-to-nearest-organism-distance, for each species across each plot (Hines and Hines, 1979).

$$I_E = (\frac{s}{\bar{x}})^2 + 1$$

where I_E = Eberhardt's index of dispersion for point-to-organism distances, s = the observed standard deviation of distances, and $\bar{x}$ = the mean of point-to-organism distances. The expected value of I_E in a random population is 1.27 – values below suggest a regular pattern, values above suggest clumping.

2.3 Fire behavior modeling

To model fire behavior based on estimated fuel structures in reburns, we used the Wildland-Urban Interface Fire Dynamics Simulator (WFDS), version 9977. WFDS version 9977 is based on Fire Dynamics Simulator (FDS) version 6, developed by the National Institute of Standards and Technology (McGrattan et al., n.d.). We chose WFDS over other modeling approaches for two reasons. First, it is a coupled fire atmospheric model that provides spatial and temporal predictions of fire behavior based on linkages between a large eddy computational fluid dynamics model and models for thermal degradation, convective and radiative heat transfer, and gas-phase combustion. This approach allows the model to capture the emergent fire behavior associated with the interactions between fuel structures, wind flow, and fire. Second, WFDS represents heterogeneity in fuel load, moisture and physical characteristics in 3-dimensions providing the capacity to capture the complex fuel dynamics that occur in borders between dramatically different cover types (Hoffman et al., 2018; Mell et al., 2009), such as those occurring between mature black spruce forests and regenerating deciduous stands (Boby et al., 2010; Cahoon et al., 2022). Further descriptions of the WFDS and FDS including verification and validation can be found in the following: (Castle et al., 2013; McGrattan et al., 2012, n.d.; McGrattan and Hostikka, n.d.; Mell, 2007; Mell et al., 2009; Mueller et al., 2014; Overholt et al., 2014; Perez-Ramirez et al., 2017; Ritter et al., 2020; Sánchez-Monroy et al., 2019).

Once-burned landscape

Average fuel Moderate fire weather	High fuel Moderate fire weather
Average fuel Extreme fire weather	High fuel Extreme fire weather

Thrice-burned landscape

Average fuel Moderate fire weather	High fuel Moderate fire weather
Average fuel Extreme fire weather	High fuel Extreme fire weather

Figure 1. Modeling Scenarios. Simulated landscapes were built using observed forest composition and structure characteristics from once-burned and thrice-burned plots, using mean values and 90th quartile values to represent an average fuel load and an extreme fuel load.

Our simulation-based experimental design was fully factorial. This included (1) fuel setups with once- and thrice-burned fuels in the latter half of the fire simulation domain (with unburned fuels in the front half). (2) Moderate or extreme fire weather. Moderate fire weather was simulated with a surface fuel moisture of 10%, open (10-m above ground level or AGL) wind speed of 4 m/s, and conifer/hardwood foliar moisture content of 97% and 109%, respectively. Extreme fire weather simulations had surface fuel moistures of 10%, open (10-m AGL) wind speeds of 8 m/s, and conifer/hardwood foliar moisture contents of 77% and 89%. We used fuel moisture metrics from the National Fuel Moisture Database (United States Forest Service 2010), using the average (across 2011–2020) monthly minimum foliar moisture content.

We generated random landscapes based on the observed densities, surface fuels, and spatial dispersion of trees for once- and thrice-burned stands. To produce a representation of the average fuel characteristics, we distributed the mean density of trees across each simulated landscape and pulled from our distributions of composition, height, and DBH to assign each tree species, live/dead status, height, and volume. To produce an extreme representation of fuel, we distributed the 90^{th} quartile density of trees across the same 800 m × 300 m landscape pulled from the same distributions of composition, height, and DBH to assign tree characteristics (code available online). In all scenarios, conifers were represented as cones, and deciduous species were represented as cylinders. To capture the transition of fire from unburned to reburned stands, we started each modeled fire ignition in a simulated black spruce stand based on measurements of the forest structure and composition in our unburned reference plots (Fig. 2).

The simulation domains spanned 560 m in the streamwise direction, 70 m in the spanwise direction, and 95 m tall. The actual tracked trees differed between scenarios because of the computational restraints produced by the high number of trees in the high-fuel scenario. The once-or three burned fuels began 360 m from the inlet of the domain at a location labelled x = 0 and extended to the outlet of the domain 200 m downwind of the transition at x = 200 m. Upwind unburned forest fuels spanned from x = -360 to x = 0 m. Inlets (x = -360 m) had wind entering, following a typical wind profile power law function ($u(z) = u(r) \times (z/z(r))^{(1/7)}$) where u(r) was either 4 m/s or 8 m/s depending on our specific simulation case and z(r) was 10 m. Wind exited at x = 200 m.

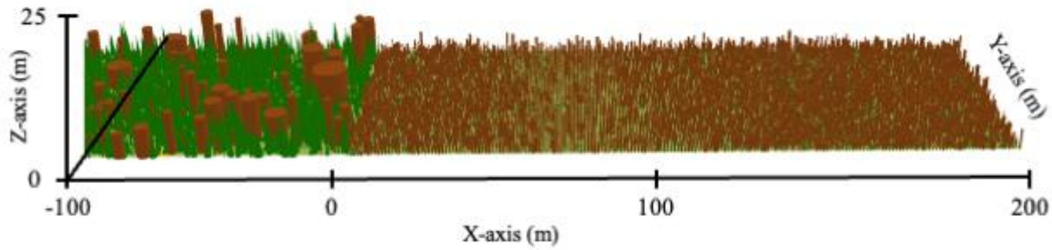

Figure 2. Example of simulated WFDS landscape. X = 0 represents the transition zone between unburned and burned landscapes. The Z-axis represents the height of the modeling domain, determined by the 90th quartile of the heights observed in the field. The Y-axis represents the width of the area tracked within the modeling domain and differs according to the model scenario: high-fuel scenarios produce too many trees to be tracked across the same space. Cones represent deciduous species, cylinders represent conifers.

We represented understory fuel loads using the combined mean values of understory vegetation weight and seedling weight per square meter. Based on observations of percent cover, we distributed two forms of surface fuels across each landscape: 1) a representative litter layer that included litter, lichen, fine fuels, and other organic materials, and 2) a litter, herb and shrub layer that included woody surface fuels.

To explore how the characteristics of potential fire behavior differed across fuel/weather/burn scenarios, we tracked the 2m AGL wind velocity (m/s) (prior to fire ignition), time of arrival (s), rate of spread (m/s), and surface and canopy fuel consumption in each simulation. Rate of spread was calculated in m/s using loess smoothing of the time of arrival for each pixel from X = 0. Time of arrival represents the first time in seconds a loss of biomass is observed in each given pixel. These metrics are directly linked to fire behavior properties that direct the subsequent total area burned, fire severity, and fire management conditions. We estimated canopy and canopy consumption in each scenario, measured as the percentage of dry mass consumed between the start and end of the simulation. Canopy fuel consumption was estimated as the average consumption of tracked trees (the number of which was determined by computational restraints) in the area of interest for each scenario. Because of the relatively low number of replications (due to processing time), we chose to analyze the results in a primarily qualitative fashion.

3. Results

3.1 Fuel Abundance

The abundance of owned woody fuel in all size classes increased with reburning, but differed across specific reburn history and size classes. Fine fuels (1- and 10-hour fuels) were most abundant in the once- and twice-burned plots, increasing by an average factor of three after one fire, decreasing by a factor of 1.6 after two fires, and increasing by a factor of two after three fires. Large fuels (1,000-hour fuels) followed a similar trend, increasing by a factor of 8 after one fire, declining after the second, and reaching a maximum average of 4.29 tons per ha after three fires. Medium fuel size classes (100-hours) increased after one fire but did not change meaningfully between reburning (Fig. 3).

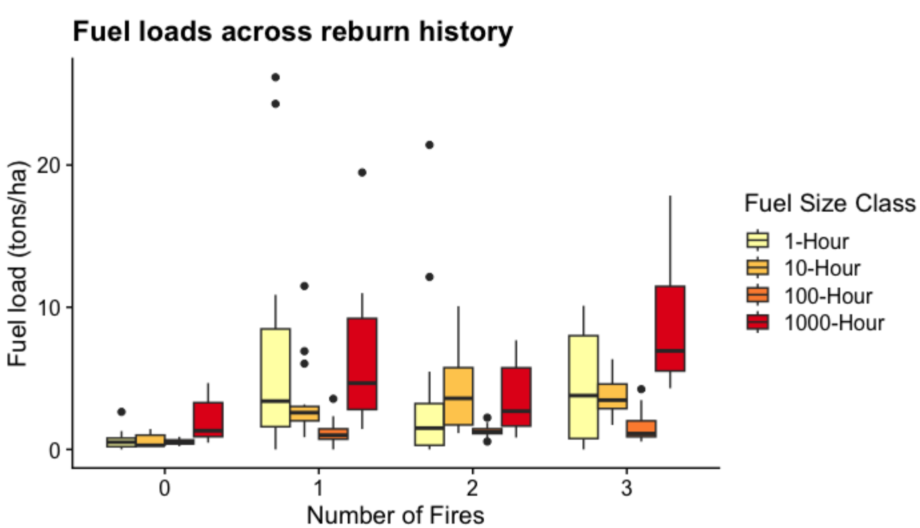

Figure 3. Average mass fuel load by fuel size classes of dead down woody debris (Tons/Ha) across years since initial fire and between sites according to size classes. Dots represent outliers.

The density and mass of standing fuels (live and dead trees) differed between the once-burned and thrice-burned plots: once-burned plots contained greater numbers of dead trees, primarily spruce, killed in the first fire. Spruce had the highest DBH in the dataset and thus contained the greatest mass. Tree height was greatest in once-burned stands, again due to the increased presence of dead spruce in the landscape (species height distributions are presented in Appendix: Fig. S1). Trees were generally less dense in the burned plots. In both the once- and thrice-burned scenarios, using the 90th quartile of tree density observations doubled the number of trees in the simulation, and roughly doubled the fuel load and density (Table 1).

Table 1. Fuel abundance and density of trees (live/dead) within burns and scenarios. DBH is the average diameter of trees, measured in centimeters. Density is the number of trees per m^2. SD stands for standard deviation. Fuel load is measured in kilograms per square meter. Bulk density is measured in kilograms per cubic meter.

Burn	Fuel Scenario	Fuel Load (Kg/m^2)	Bulk Density (Kg/m3)	Status	DBH (cm)	Density (trees/m^2)
1x	Mean	0.02	0.01	Live	0.7 (SD 0.5)	0.8
				Dead	3.2 (SD 2.7)	0.8
	High	0.03	0.017	Live	0.7 (SD 0.5)	1.4
				Dead	3.2 (SD 2.7)	1.4
3x	Mean	0.05	0.013	Live	1.2 (SD 0.9)	0.6
				Dead	0.9 (SD 0.8)	0.6
	High	0.11	0.029	Live	1.2 (SD 0.9)	1.4
				Dead	0.9 (SD 0.75)	1.4

3.2 Fuel Structure

Surface fuels were less connected in the thrice-burned plots than in the once-burned plots (Fig. 4). Once-burned plots had greater surface fuel cover and fuel loads than thrice-burned stands (Table 2). Thrice-burned plots contained high amounts of litter patches without surface fuels (Fig. 4).

Table 2. Characteristics of surface fuel and ground cover between once-burned and thrice-burned plots.

Burn	Fuel Type	% Cover	Height (m)	Moisture (%)	Bulk Density (kg/m^3)	Load (kg/m^2)
1	Litter	13.9%	0.04	20	2	0.02
	Litter, Herbs, Shrubs	86.2%	0.243	38	3.64	0.0668
3	Litter	61.1%	0.04	20	2	0.02
	Litter, herbs, shrubs	38.9%	0.243	65	10.2	0.0238

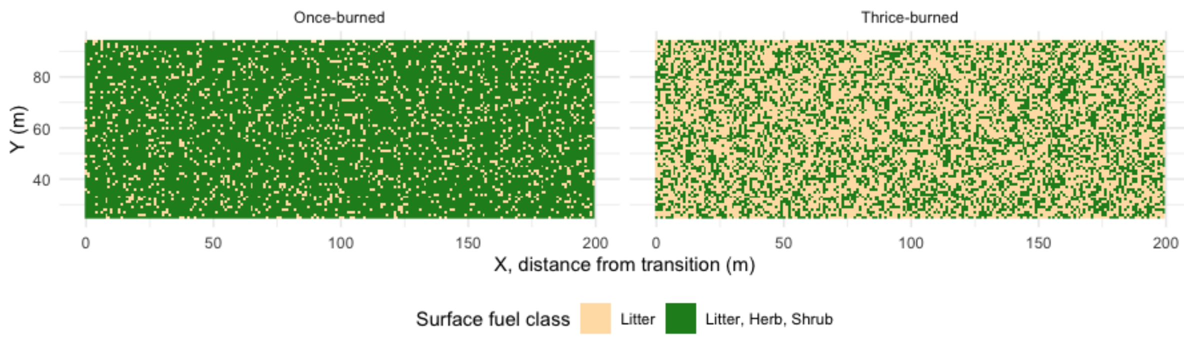

Figure 4. Surface fuels across once- and thrice-burned simulated landscapes. X = 0 indicates the transition zone. Surface fuels are split into two classes:1) litter only, shown in tan, where leaves, lichen, moss, and organic material are present, but not understory vegetation; and 2) litter, herbs, and shrubs, shown in green, where herbs and woody shrubs are present on top of the existing litter layer.

Trees of all species displayed a non-random spatial distribution (Fig. 5). While Eberhardt's index for all species was above the 1.27 random pattern threshold, the spatial dispersion of species differed between once-burned and thrice-burned plots. Variability among species was the greatest in the once- and thrice-burned plots. Eberhardt's index values for aspen in particular show the greatest change across burn history, increasing from 1.37 to 1.71 to 2.69

after three fires, indicating a more clumped spatial pattern.

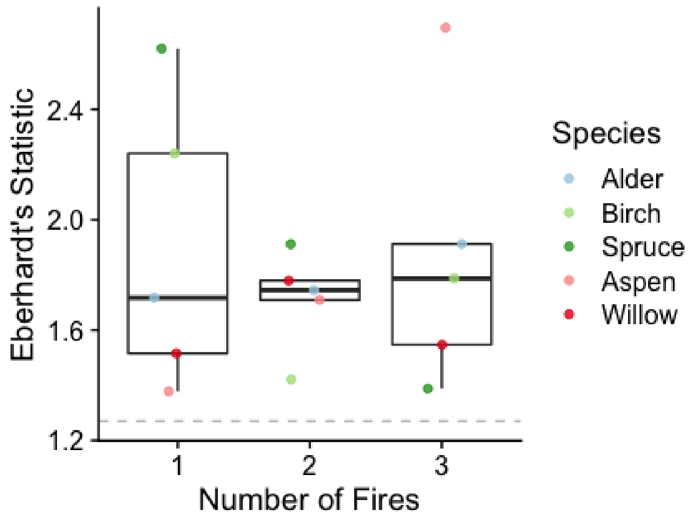

Figure 5. Eberhardt’s index (a metric of dispersion based on random point-to-nearest-organism distances) across reburn history. The expected value in a random population is 1.27; values below suggest a regular pattern and values above suggest clumping.

3.3 Modeled Fire Behavior

Simulations show a typical forest canopy flow upwind of the transition point (x = 0) consisting of a turbulent field with sweeps and jet formation acting as the primary mechanism for upward and downwards air movement. As the flow approaches the transition point, there is a reversal of the canopy flow direction associated with the detachment of the above canopy flow and void in pressure on the upwind edge of the mature black spruce canopy. After 50–100 m, the flow above the canopy flow reattaches, resulting in a significant increase in the wind velocity (Fig 8). Wind speeds were slightly higher in mean fuel scenarios than in high fuel scenarios, regardless of the burn history. The primary difference between burn scenarios is the slightly faster wind speeds present towards the edge of the once-burned simulated landscape (x = 100 to 200, wind speeds reach 6 m/s, Fig. 6A) compared to the thrice-burned landscape (in the same region, wind speeds reach 4 m/s; Fig. 6B).

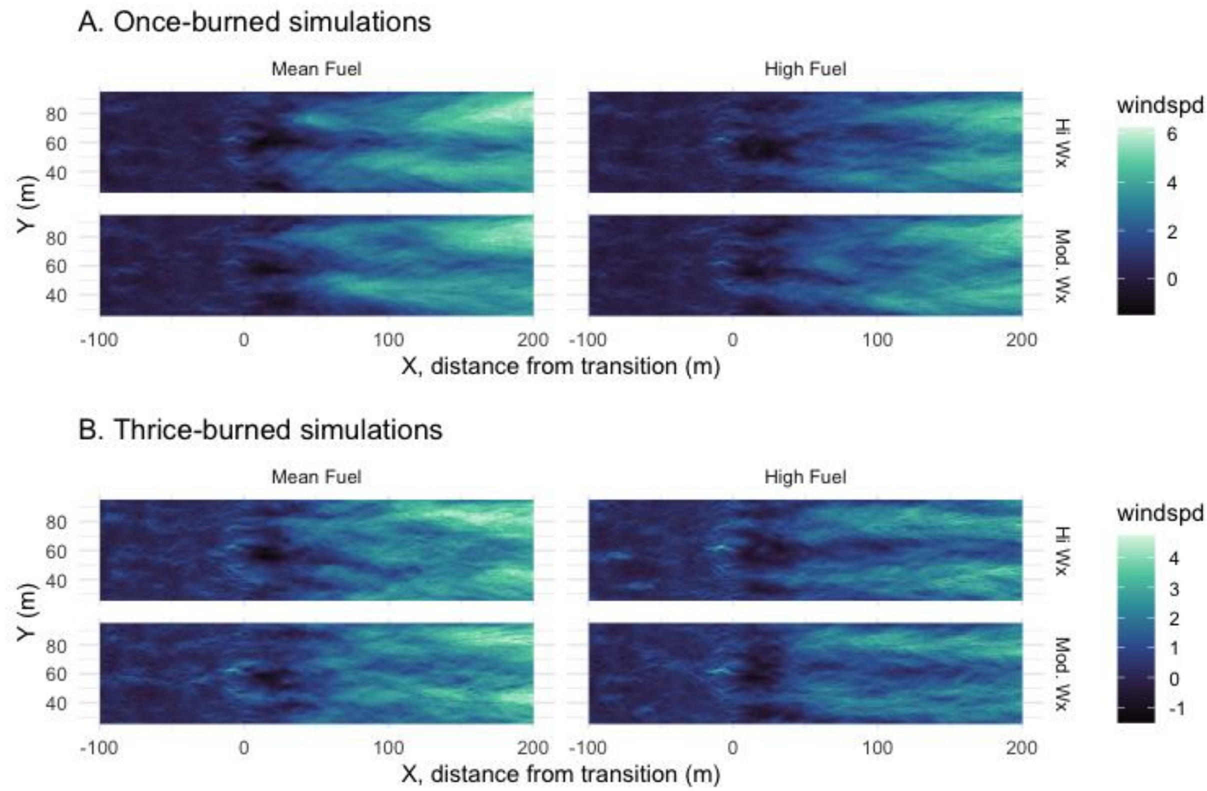

Figure 6. Wind speed across scenario landscapes (in meters per seconds). X = -100 to 0 is the mature unburned simulated landscape, X = 0 is the start of the transition point, and X = 0 to 200 is the reburned simulated landscape. A) Wind speed across all scenarios of once-burned simulated landscapes. B) Wind speed across all scenarios of simulated thrice-burned landscapes.

Out of the eight total scenarios, only one (once-burned, mean fuel, and extreme weather) experienced sustained fire spread across the majority of the domain. In all other scenarios, fire burned into the reburned landscape and halted within 50–75 m beyond the transition point x = 0. Both the once-burned and thrice-burned scenarios burned in WFDS, but fire behavior differed greatly between reburn histories. In both the once-burned and thrice-burned landscapes, bare patches of ground seemed to prevent fire spread, as demonstrated in both the high-fuel + extreme weather scenarios, in which the fire forked in two directions owing to the presence of a bare patch (Fig. 7A, Fig. 7B).

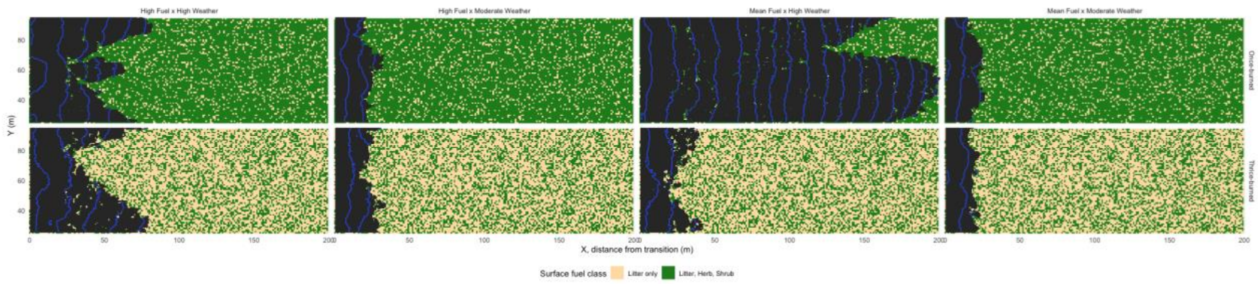

Figure 7. Time of arrival of fire, measured as the first measurable loss of biomass within a given pixel, shown in two dimensions. X = 0 at the bottom left indicates the start of the burned fuels and the beginning of the transition between the mature and burned landscapes. Contours represent 10 second intervals. A) Once-burned landscape. B) Thrice-burned landscape.

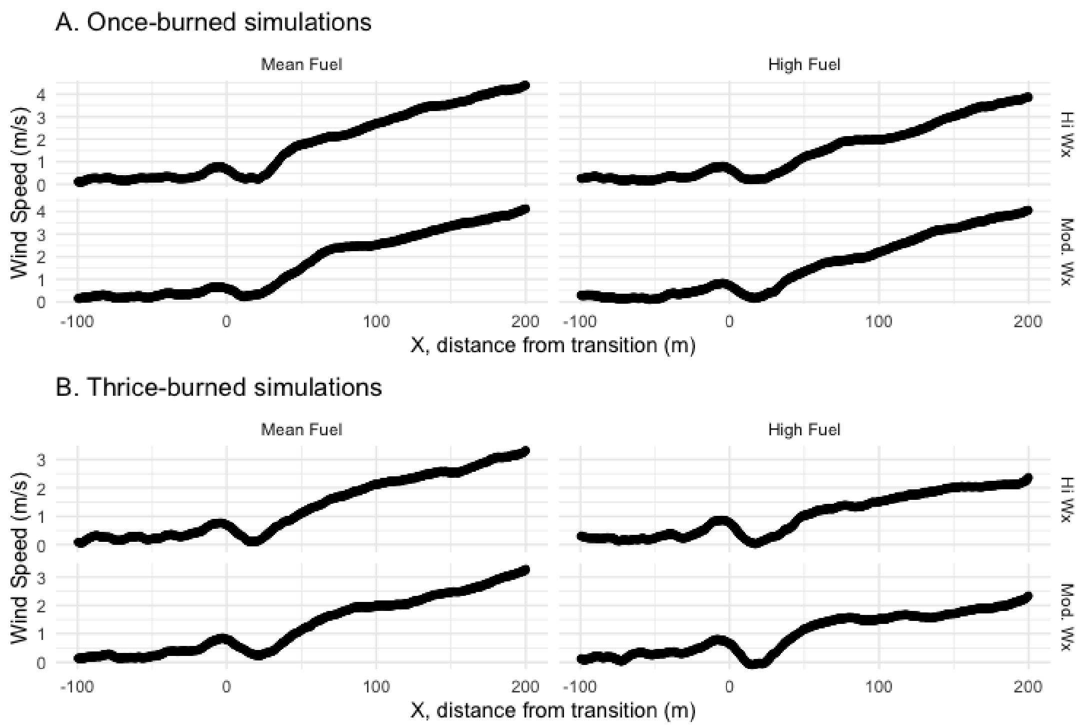

Figure 8. Wind speed (in meters per second) averaged across the y-axis of landscape scenarios. “Hi Wx” stands for the extreme weather conditions and “Mod. Wx” for the moderate scenario of fire weather conditions. A) Windspeed across all scenarios of once-burned simulated landscapes. B) Windspeed across all scenarios of thrice-burned simulated landscapes.

Within each scenario, trends in the rate of spread of the fire initially followed trends in wind speed; as wind speed dropped after the transition point at x = 0 (Fig. 8), the rate of spread declined in all scenarios (Fig. 9). As wind speed begins to pick back up with increasing distance from the transition point, rate of spread does as well. However, across all scenarios, the rate of spread and wind eventually diverged. While wind speed continued to increase with distance from the transition point in all scenarios, only the once-burned, mean fuel, and extreme fire weather scenarios continued to burn past 50-75 meters beyond the transition point.

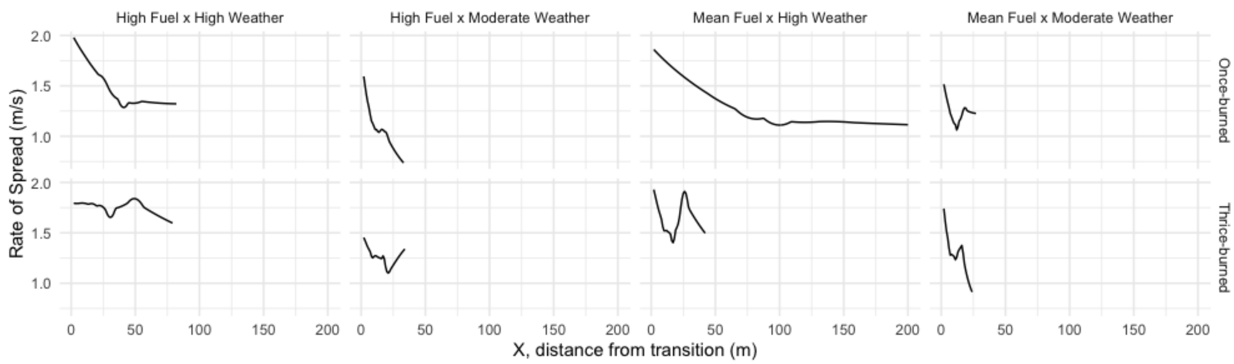

Figure 9. Rate of fire spread, in meters per second, across 200 meters of X beginning with the transition from simulated mature to reburned landscapes for each fuel/weather/burn scenario.

3.4 Modeled Fire Effects

Canopy consumption was greatest in the once-burned, mean fuel, and extreme weather scenarios (Fig. 10); again, it was the only scenario to burn past 75 m beyond the transition point (x = 0). All other scenarios displayed high canopy consumption (< 75%) within the first 25 m of combustion before dropping to 0% by the first 40 m of the reburned domain (Fig. 11).

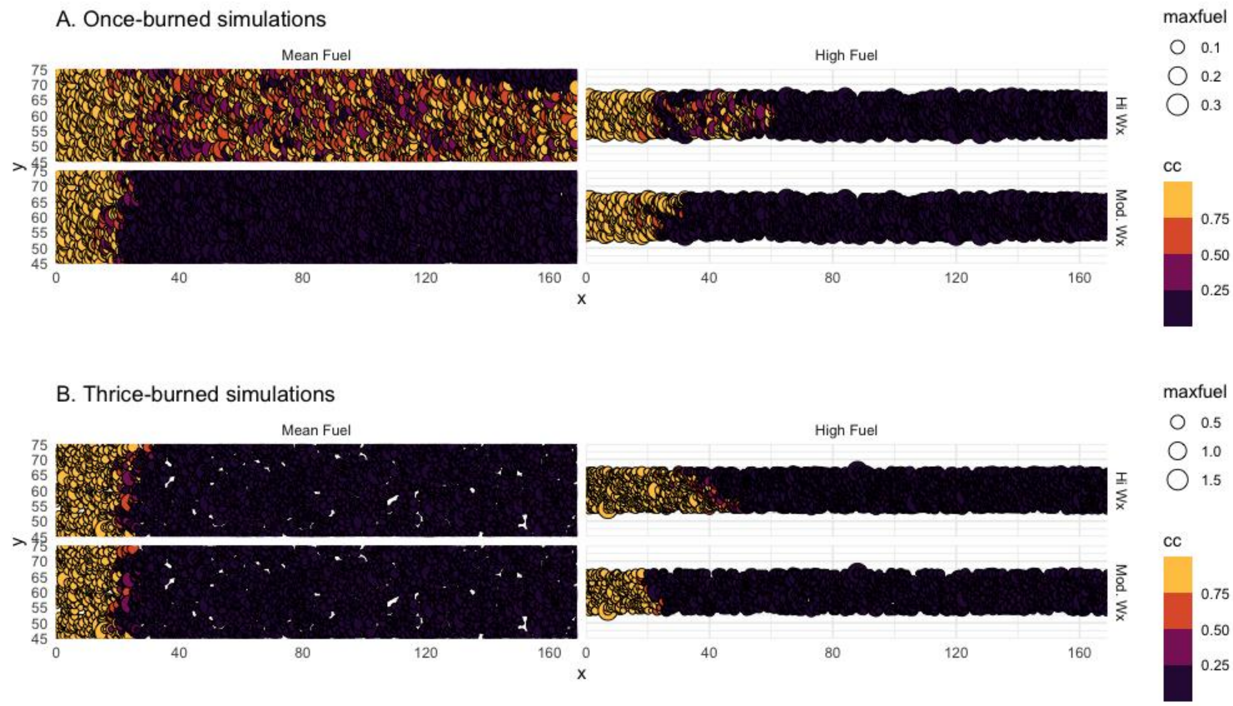

Figure 10. Two-dimensional canopy consumption between 1-time and three-time burns and across median and high-fuel scenarios. X of 0 at the bottom left indicates the start of the burned fuels and the beginning of the transition between mature and burned landscapes. High-fuel scenarios contain fewer trees owing to the computational limits to the number of trees that can be tracked in WFDS (the modeling domain remained consistent, however).

The average crown consumption was close to zero percent within 30 – 40 m past the transition zone in all thrice-burned landscapes (Fig. 11).

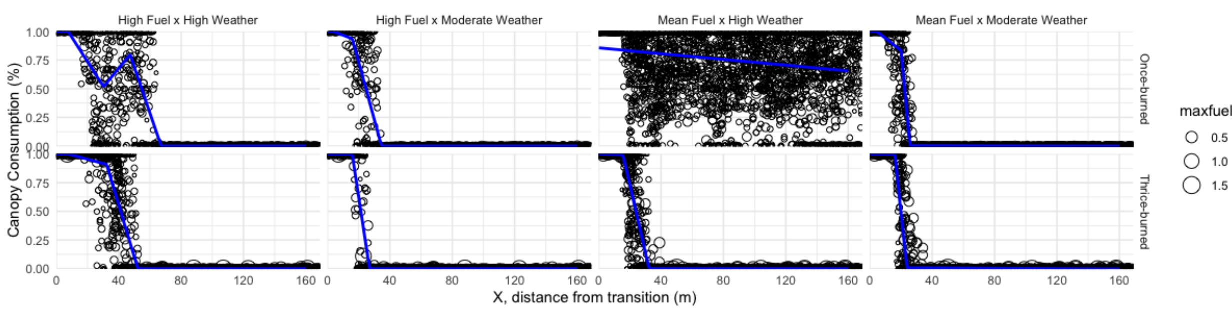

Figure 11. Crown consumption across 1-time and 3-time burns and median and high-fuel scenarios. Circles represent the difference between the starting crown mass and ending crown mass, with larger circles indicating a larger difference. Blue line represents the average.

4. Discussion

Fuel abundance increased across reburn-history, particularly the fine and large fuels. The connectivity of both surface and canopy fuels declined across reburned landscapes; thrice-burned trees displayed the most clumped spatial pattern, and the most abundant ground cover in thrice-burned landscapes was bare litter.

Once-burned landscapes displayed a greater rate of spread and consumption than thrice-burned landscapes; fire spread was rarely sustained 50 m beyond the transition point in thrice-burned simulations, even under high fuel and extreme weather conditions. Under the conditions tested, this indicates fuel constraints may not be overcome by fire weather in thrice-burned landscapes. This finding is consistent with the results of other models applied in Interior Alaska: processed-based models like the University of Virginia Forest Model Enhanced (UVAFME) found that declines in fuel abundance led to lower fire severity and intensity in stands with greater deciduous presence (Foster et al., 2022). One element that remains unclear is the relative importance of fuel abundance vs. fuel connectivity; untangling the roles of each individual fuel characteristic is critical to anticipating future fire behavior, but difficult under our current limited understanding of fire propagation(Hanan et al., 2022; Werth et al., 2011).

Transition zones and differences in modeled fire behavior between two types of fuels (i.e., unburned vs. burned or structure vs. wildland) are observable in a variety of ecosystem types. WFDS simulations of red pine and other forest types in the western US displayed transition zones from 6 m to 300 m (Ritter et al., 2022). Prior to this, transition zones between burned and unburned forests in the interior have not been simulated using a combustion model, but have been documented by fire managers across the state. Our transition zone was 50-75 meters, given that we did not observe a consistent rate of spread in the majority of scenarios more than 75 m from the transition zone.

Potential key dynamics of fire behavior in boreal forests are not fully represented in WFDS. More specifically WFDS does not include soil organic layers or coarse woody debris, which are important sources of smoldering fires in the boreal. Although we do not expect these fuels to play a significant role in fire spread over the temporal scales simulated, they may be important on a larger scale. Given the emerging nature of continued short-interval reburning, there are still relatively few documented sites of twice- and thrice-burned landscapes in the Interior. Additional empirical observations of repeat reburning will help inform our understanding of potential future fire behavior in reburned stands (and thus the strength and/or duration of a negative deciduous feedback).

Our simulated reburned landscapes were based on the observed characteristics of 15-year-old regenerated stands. Regional analysis of the frequency of reburning suggests that self-regulating feedback persists in the first 20 years after a fire (Buma et al., 2022), which is consistent with our findings. Our observation that once-burned landscapes with average fuel abundance burned under extreme weather conditions suggests that self-regulating feedbacks may be overcome by extreme fire weather conditions in stands that have burned once, which would allow for continued reburning; however, a threshold may exist in fuel abundance or connectivity that prevents fire spread in thrice-burned landscapes.

The presence of less-flammable deciduous species has been invoked as a landscape management solution to boreal warming (Astrup et al., 2018), based on paleoecological evidence of declining fire activity found alongside increases in the presence of birch pollen (Brubaker et al., 2009; Kelly et al., 2013). Our finding that simulated fire spread did not occur in thrice-burned landscapes, even under extreme conditions, suggests that fuel constraints outweigh fire weather conditions, at least during the initial decades of post-fire regeneration.

5. Acknowledgements

This study was funded by support from the NSF Polar Services Office (NSF-OPP-1903231) and a Graduate Innovation Award from the Joint Fire Science Program (ID 19-1-01-43). We are grateful to Vishnusai Kodicherla, Kyle Martini, Kristin Olson, Pauline Allen, and Teagan Furbish for their help in the field.

6. References

Astrup, R., Bernier, P.Y., Genet, H., Lutz, D.A., others, 2018. A sensible climate solution for the boreal forest. Nat Clim Chang.

Atchley, A.L., Linn, R., Jonko, A., Hoffman, C., Hyman, J.D., Pimont, F., Sieg, C., Middleton, R.S., 2021. Effects of fuel spatial distribution on wildland fire behaviour. Int J Wildland Fire 30, 179.

Balshi, M.S., Mcguire, A.D., Duffy, P., Flannigan, M., Kicklighter, D.W., Melillo, J., 2009. Vulnerability of carbon storage in North American boreal forests to wildfires during the 21st century. Glob. Change Biol. 15, 1491–1510. https://doi.org/10.1111/j.1365-2486.2009.01877.x

Barrett, K., Loboda, T., McGuire, A.D., Genet, H., Hoy, E., Kasischke, E., 2016. Static and dynamic controls on fire activity at moderate spatial and temporal scales in the Alaskan boreal forest. Ecosphere 7, e01572.

Binkley, Lousier, Cromack, 1984. Ecosystem effects of Sitka alder in a Douglas-fir plantation. For. Sci. 30, 26–35.

Boby, L.A., Schuur, E.A.G., Mack, M.C., Verbyla, D., Johnstone, J.F., 2010. Quantifying fire severity, carbon, and nitrogen emissions in Alaska's boreal forest. Ecol. Appl. 20, 1633–1647. https://doi.org/10.1890/08-2295.1

Bond-Lamberty, B., Wang, C., Gower, S.T., 2002. Aboveground and belowground biomass and sapwood area allometric equations for six boreal tree species of northern Manitoba 32, 10.

Brown, J.K., 1974. Handbook for inventorying downed woody material (No. 24). US Department of Agriculture, Forest Service, Intermountain Forest and Range Experiment Station.

Brubaker, L.B., Higuera, P.E., Rupp, T.S., Olson, M.A., Anderson, P.M., Hu, F.S., 2009. Linking sediment-charcoal records and ecological modeling to understand causes of fire-regime change in boreal forests. Ecology 90, 1788–1801. https://doi.org/10.1890/08-0797.1

Buma, B., Hayes, K., Weiss, S., Lucash, M., 2022. Short-interval fires increasing in the Alaskan boreal forest as fire self-regulation decays across forest types. Sci. Rep. 12, 4901. https://doi.org/10.1038/s41598-022-08912-8

Cahoon, S.M.P., Sullivan, P.F., Gray, A.N., 2022. Interactions among wildfire, forest type and landscape position are key determinants of boreal forest carbon stocks. J Ecol.

Castle, D., Mell, W.E., Miller, F.J., 2013. Examination of the wildland-urban interface fire dynamics simulator in modeling of laboratory-scale surface-to-crown fire transition.

Eckdahl, J.A., Kristensen, J.A., Metcalfe, D.B., 2022. Climatic variation drives loss and restructuring of carbon and nitrogen in boreal forest wildfire. Biogeosciences 19, 2487–2506. https://doi.org/10.5194/bg-19-2487-2022

Foster, A.C., Wang, J.A., Frost, G.V., Davidson, S.J., Hoy, E., Turner, K.W., Sonnentag, O., Epstein, H., Berner, L.T., Armstrong, A.H., others, 2022. Disturbances in North American boreal forest and Arctic tundra: impacts, interactions, and responses. Environ. Res. Lett. 17, 113001.

Hanan, E.J., Kennedy, M.C., Ren, J., Johnson, M.C., Smith, A.M.S., 2022. Missing Climate Feedbacks in Fire Models: Limitations and Uncertainties in Fuel Loadings and the Role

of Decomposition in Fine Fuel Accumulation. J. Adv. Model. Earth Syst. 14, e2021MS002818. https://doi.org/10.1029/2021MS002818
Hart, S.J., Henkelman, J., McLoughlin, P.D., Nielsen, S.E., Truchon-Savard, A., Johnstone, J.F., 2019. Examining forest resilience to changing fire frequency in a fire-prone region of boreal forest. Glob. Change Biol. 25, 869–884. https://doi.org/10.1111/gcb.14550
Hayes, K., Buma, B., 2021. Effects of short-interval disturbances continue to accumulate, overwhelming variability in local resilience. Ecosphere 12. https://doi.org/10.1002/ecs2.3379
Hély, C., Bergeron, Y., Flannigan, M.D., 2000. Effects of stand composition on fire hazard in mixed-wood Canadian boreal forest. J. Veg. Sci. 11, 813–824. https://doi.org/10.2307/3236551
Higuera, P.E., Brubaker, L.B., Anderson, P.M., Brown, T.A., Kennedy, A.T., Hu, F.S., 2008. Frequent Fires in Ancient Shrub Tundra: Implications of Paleorecords for Arctic Environmental Change. PLoS ONE 3, e0001744. https://doi.org/10.1371/journal.pone.0001744
Hines, W.G.S., Hines, R.J.O., 1979. The Eberhardt statistic and the detection of nonrandomness of spatial point distributions. Biometrika 66, 73–79. https://doi.org/10.1093/biomet/66.1.73
Hoecker, T.J., Higuera, P.E., 2019. Forest succession and climate variability interacted to control fire activity over the last four centuries in an Alaskan boreal landscape. Landsc Ecol 34, 227–241.
Hoffman, C., Morgan, P., Mell, W., Parsons, R., Strand, E.K., Cook, S., 2012. Numerical Simulation of Crown Fire Hazard Immediately after Bark Beetle-Caused Mortality in Lodgepole Pine Forests. For. Sci. 58, 178–188. https://doi.org/10.5849/forsci.10-137
Hoffman, C., Sieg, C., Linn, R., Mell, W., Parsons, R., Ziegler, J., Hiers, J., 2018. Advancing the Science of Wildland Fire Dynamics Using Process-Based Models. Fire 1, 32. https://doi.org/10.3390/fire1020032
Hoffman, C.M., Morgan, P., Mell, W., Parsons, R., Strand, E., Cook, S., 2013. Surface Fire Intensity Influences Simulated Crown Fire Behavior in Lodgepole Pine Forests with Recent Mountain Pine Beetle-Caused Tree Mortality. For. Sci. 59, 390–399. https://doi.org/10.5849/forsci.11-114
Johnstone, J.F., Celis, G., Chapin, F.S., Hollingsworth, T.N., Jean, M., Mack, M.C., 2020. Factors shaping alternate successional trajectories in burned black spruce forests of Alaska. Ecosphere 11. https://doi.org/10.1002/ecs2.3129
Johnstone, J.F., Chapin, F.S., 2006. Effects of Soil Burn Severity on Post-Fire Tree Recruitment in Boreal Forest. Ecosystems 9, 14–31. https://doi.org/10.1007/s10021-004-0042-x
Johnstone, J.F., Hollingsworth, T.N., Chapin, F.S., Mack, M.C., 2010. Changes in fire regime break the legacy lock on successional trajectories in Alaskan boreal forest. Glob. Change Biol. 16, 1281–1295. https://doi.org/10.1111/j.1365-2486.2009.02051.x
Kasischke, E.S., Verbyla, D.L., Rupp, T.S., others, 2010. Alaska's changing fire regime—implications for the vulnerability of its boreal forests. J. For. ….
Kelly, R., Chipman, M.L., Higuera, P.E., Stefanova, I., Brubaker, L.B., Hu, F.S., 2013. Recent burning of boreal forests exceeds fire regime limits of the past 10,000 years. Proc. Natl. Acad. Sci. 110, 13055–13060. https://doi.org/10.1073/pnas.1305069110

Lund, M.T., Nordling, K., Gjelsvik, A.B., Samset, B.H., 2023. The influence of variability on fire weather conditions in high latitude regions under present and future global warming. Environ. Res. Commun. 5, 065016. https://doi.org/10.1088/2515-7620/acdfad

Mack, M.C., Walker, X.J., Johnstone, J.F., Alexander, H.D., Melvin, A.M., Jean, M., Miller, S.N., 2021. Carbon loss from boreal forest wildfires offset by increased dominance of deciduous trees. Science 372, 280–283.

McGrattan, K., Hostikka, S., n.d. Verification and Validation Process of a Fire Model.

McGrattan, K., Hostikka, S., McDermott, R., Floyd, J., Weinschenk, C., Overholt, K., n.d. Fire Dynamics Simulator User's Guide. NIST Spec. Publ.

McGrattan, K., McDermott, R., Floyd, J., Hostikka, S., Forney, G., Baum, H., 2012. Computational fluid dynamics modelling of fire. Int. J. Comput. Fluid Dyn. 26, 349–361. https://doi.org/10.1080/10618562.2012.659663

Mell, W., 2007. Modeling wildland and wildland-urban interface fires.

Mell, W., Maranghides, A., McDermott, R., Manzello, S.L., 2009. Numerical simulation and experiments of burning douglas fir trees. Combust. Flame 156, 2023–2041. https://doi.org/10.1016/j.combustflame.2009.06.015

Mell, W., McNamara, D., Maranghides, A., McDermott, R., Forney, G., Hoffman, C., Ginder, M., 2011. COMPUTER MODELLING OF WILDLAND-URBAN INTERFACE FIRES 13.

Mell, W.E., McDermott, R.J., Forney, G.P., Hoffman, C., Ginder, M., 2010. Wildland Fire Behavior Modeling: Perspectives, New Approaches and Applications 17.

Mueller, E., Mell, W., Simeoni, A., 2014. Large eddy simulation of forest canopy flow for wildland fire modeling. Can. J. For. Res. 44, 1534–1544. https://doi.org/10.1139/cjfr-2014-0184

Overholt, K.J., Kurzawski, A.J., Cabrera, J., Koopersmith, M., Ezekoye, O.A., 2014. Fire behavior and heat fluxes for lab-scale burning of little bluestem grass. Fire Saf. J. 67, 70–81. https://doi.org/10.1016/j.firesaf.2014.05.007

Parks, S.A., Holsinger, L.M., Miller, C., others, 2015. Wildland fire as a self-regulating mechanism: the role of previous burns and weather in limiting fire progression. Ecological.

Parsons, R., Linn, R., Pimont, F., Hoffman, C., Sauer, J., Winterkamp, J., Sieg, C., Jolly, W., 2017. Numerical investigation of aggregated fuel spatial pattern impacts on fire behavior. Land Basel 6, 43.

Perez-Ramirez, Y., Mell, W.E., Santoni, P.A., Tramoni, J.B., Bosseur, F., 2017. Examination of WFDS in Modeling Spreading Fires in a Furniture Calorimeter. Fire Technol. 53, 1795–1832. https://doi.org/10.1007/s10694-017-0657-z

Ritter, S.M., Hoffman, C.M., Battaglia, M.A., Jain, T.B., 2022. Restoration and fuel hazard reduction result in equivalent reductions in crown fire behavior in dry conifer forests. Ecol. Appl. 32, e2682. https://doi.org/10.1002/eap.2682

Ritter, S.M., Hoffman, C.M., Battaglia, M.A., Stevens-Rumann, C.S., Mell, W.E., 2020. Fine-scale fire patterns mediate forest structure in frequent-fire ecosystems. Ecosphere 11, e03177.

Sánchez-Monroy, X., Mell, W., Torres-Arenas, J., Butler, B.W., 2019. Fire spread upslope: Numerical simulation of laboratory experiments. Fire Saf. J. 108, 102844. https://doi.org/10.1016/j.firesaf.2019.102844

Stocks, B.J., Lynham, T.J., Lawson, B.D., Alexander, M.E., Van Wagner, C.E., McAlpine, R.S., Dubé, D.E., 1989. Canadian Forest Fire Danger Rating System: An overview. Chron 65, 258–265.

Turquety, S., Logan, J.A., Jacob, D.J., Hudman, R.C., Leung, F.Y., Heald, C.L., Yantosca, R.M., Wu, S., Emmons, L.K., Edwards, D.P., Sachse, G.W., 2007. Inventory of boreal fire emissions for North America in 2004: Importance of peat burning and pyroconvective injection. J Geophys Res 112.

Veraverbeke, S., Rogers, B.M., Goulden, M.L., Jandt, R.R., Miller, C.E., Wiggins, E.B., Randerson, J.T., 2017. Lightning as a major driver of recent large fire years in North American boreal forests. Nat. Clim. Change 7, 529–534. https://doi.org/10.1038/nclimate3329

Werth, P., Potter, B., Clements, C., Finney, M., Forthofer, J., McAllister, S., Goodrick, S., Alexander, M., Cruz, M., 2011. Synthesis of Knowledge of Extreme Fire Behavior: Volume I for Fire Managers. JFSP Synth. Rep.

Ziegler, J.P., Hoffman, C.M., Collins, B.M., Knapp, E.E., Mell, W. (Ruddy), 2021. Pyric tree spatial patterning interactions in historical and contemporary mixed conifer forests, California, USA. Ecol. Evol. 11, 820–834. https://doi.org/10.1002/ece3.7084

Ziegler, J.P., Hoffman, C.M., Collins, B.M., Long, J.W., Dagley, C.M., Mell, W., 2020. Simulated Fire Behavior and Fine-Scale Forest Structure Following Conifer Removal in Aspen-Conifer Forests in the Lake Tahoe Basin, USA. Fire 3, 51. https://doi.org/10.3390/fire3030051